A stereoscopic view of the packing of the ET molecules is presented in Fig. 5. This arrangement is of the β-type (Williams et al., 1987). As commonly observed in the quasi-two-dimensional type of compounds the most significant intermolecular S$\cdots$S contacts are established between adjacent stacks.

References

B. A. FRENZ & ASSOCIATES INC. (1985). SDP Structure Determination Package. College Station, Texas, USA, and Enraf–Nonius, Delft, The Netherlands.
BENCHARIF, M. & OUAHAB, L. (1988). Acta Cryst. C44, 1514–1516.
Enraf–Nonius (1985). CAD-4 Program. Version 4.1. Enraf–Nonius, Delft, The Netherlands.
FETTOUHI, M., OUAHAB, L., GRANDJEAN, D. & TOUPET, L. (1992). Acta Cryst. B48, 275–280.
GARRIGOU-LAGRANGE, C., OUAHAB, L., GRANDJEAN, D. & DELHAES, P. (1990). Synth. Met. 35, 9–16.
KAWAMOTO, A., TANAKA, M. & TANAKA, J. (1991). Bull. Chem. Soc. Jpn, 64, 3160–3162.
KOBAYASHI, H., KOBAYASHI, A., SASAKI, Y., SAÏTO, G. & INOKUCHI, H. (1986). Bull. Chem. Soc. Jpn, 59, 301–302.
MALLAH, T., HOLLIS, C., BOTT, S., KURMOO, M., DAY, P., ALLAN, M. & FRIEND, R. H. (1990). J. Chem. Soc. Dalton Trans. 3, 859–865.
OUAHAB, L., PADIOU, J., GRANDJEAN, D., GARRIGOU-LAGRANGE, C., DELHAES, P. & BENCHARIF, M. (1989). J. Chem. Soc. Chem. Commun. pp. 1038–1041.
OUAHAB, L., TRIKI, S., GRANDJEAN, D, BENCHARIF, M., GARRIGOU-LAGRANGE, C. & DELHAES, P. (1990). Lower-Dimensional Systems and Molecular Electronics, Vol. 284, edited by R. M. METZGER, pp. 185–190. New York. Plenum Press.
SCHULTZ, A. J., BENO, M. A., GEISER, U., WANG, H. H., KINI, A. M., WILLIAMS, J. M. & WHANGBO, M. H. (1991). J. Solid State Chem. 94, 352–361.
TRIKI, S., OUAHAB, L., GRANDJEAN, D. & FABRE, J. M. (1991). Acta Cryst. C47, 645–648.
WALKER, N. & STUART, D. (1983). Acta Cryst. A39, 158–166.
WILLIAMS, J. M., WANG, H. H., EMGE T. J., GEISER, U., BENO, M. A., LEUNG, P. C. W., CARLSON, K. D., THORN, R. J., SCHULTZ A. J. & WHANGBO, M. H. (1987). Prog. Inorg. Chem. 35, 51–218.

X-ray Diffraction Study of the Ferroelectric Phase Transition of (CH₃)₄NCdBr₃ (TMCB)

BY G. AGUIRRE-ZAMALLOA

Laboratoire de Spectroscopie Moléculaire et Cristalline, URA 124, CNRS, Université de Bordeaux I, 33405 Talence CEDEX, France

G. MADARIAGA

Departamento de Física de la Materia Condensada, Facultad de Ciencias, Universidad del País Vasco, Apdo. 644, 48080 Bilbao, Spain

M. COUZI

Laboratoire de Spectroscopie Moléculaire et Cristalline, URA 124, CNRS, Université de Bordeaux I, 33405 Talence CEDEX, France

AND T. BRECZEWSKI

Departamento de Física Aplicada II, Facultad de Ciencias, Universidad del País Vasco, Apdo. 644, 48080 Bilbao, Spain

Abstract

The crystal structure of tetramethylammonium tribromocadmate (II), [N(CH₃)₄][CdBr₃] (TMCB), has been studied at 295 and 85 K, in order to analyze the structural changes connected with the improper para–ferroelectric phase transition occurring at ~ 160 K. The space group of the paraelectric (room-temperature) phase is $P6_3/m$ and that of the ferroelectric (low-temperature) phase is $P6_1$–$P6_5$. Final agreement factors are R $(wR) = 0.062$ (0.075) and R $(wR) = 0.029$ (0.038) for the data collected at 295 and 85 K respectively. It is shown that this phase transition is related to an orientational order–disorder process of the tetramethylammonium (TMA) groups, which leads to a tripling of the lattice constant along the c (hexad) direction; this process can be described by the freezing of a pseudo-spin coordinate defined in the frame of a Frenkel-type model. In addition, the helical-type structure found for the ferroelectric

phase occurs as a result of a bi-linear coupling of this pseudo-spin variable with the transverse acoustic mode at point $\Delta(0,0,\frac{1}{3})$. The spontaneous polarization comes from the combination of a small distortion of the ordered TMA groups and an anti-translation of $CdBr_3$ octahedra chains against the TMA groups. Crystal data: $M_r = 426.27$, $\lambda(Mo\ K\alpha) = 0.7107$ Å. At 295 K: $P6_3/m$, $Z = 2$, $F(000) = 392$, $a = 9.388\ (2)$, $c = 6.991\ (5)$ Å, $V = 533.6\ (6)$ Å^3, $D_x = 2.653\ (3)$ g cm^{-3}, $\mu = 131.03$ cm^{-1}. At 85 K: $P6_1(P6_5)$, $Z = 6$, $F(000) = 1176$, $a = 9.219\ (4)$, $c = 20.86\ (1)$ Å, $V = 1536\ (2)$ Å^3, $D_x = 2.765\ (4)$ g cm^{-3}, $\mu = 136.56$ cm^{-1}.
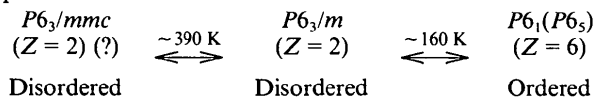
1. Introduction

The crystals with general formula $N(CH_3)_4[MX_3]$ (M = Mn, Cd; X = Cl, Br) are hexagonal at room temperature, with space group $P6_3/m$ ($Z = 2$) (Morosin & Graeber, 1967; Morosin, 1972; Alcock & Holt, 1978; Visser & McIntyre, 1989; Krishnan, Dou & Weiss, 1991).

The structure has a strong one-dimensional character; it is built up from infinite linear chains of face-sharing MX_6 octahedra, and the space between chains is occupied by the tetramethylammonium (TMA) groups, exhibiting orientational disorder of dynamic nature (Mangum & Utton, 1972; Tsang & Utton, 1976; Guillaume, Couzi & Bée, 1992).

These compounds undergo a number of structural phase transitions, governed essentially by the reorientational dynamics of the TMA groups, and leading to different ordered low-temperature phases, ferroelastic in the case of $(TMA)MnCl_3$ (TMMC) and $(TMA)CdCl_3$ (TMCC) (see, e.g., Peercy, Morosin & Samara, 1973; Braud, Couzi, Chanh, Courseille, Gallois, Hauw & Meresse, 1990; Braud, Couzi, Chanh & Gómez-Cuevas, 1990; Braud, Couzi & Chanh, 1990, and references therein), or ferroelec- tric in the case of $(TMA)CdBr_3$ (TMCB) (Gesi, 1990).

To our knowledge (Vanek, Havranova, Smutny & Brezina, 1990; Gesi, 1990; Aguirre-Zamalloa, Couzi, Chanh & Gallois, 1990), TMCB undergoes two phase transitions:

$P6_3/mmc$		$P6_3/m$		$P6_1(P6_5)$
$(Z = 2)$ (?)	$\underset{\sim 390\ K}{\rightleftharpoons}$	$(Z = 2)$	$\underset{\sim 160\ K}{\rightleftharpoons}$	$(Z = 6)$
Disordered		Disordered		Ordered

The high-temperature transition is of second order (Vanek et al., 1990) and probably leads to the proto- type structure of this family of compounds, with space group $P6_3/mmc$ (Braud, Couzi, Chanh, Courseille et al., 1990). At lower temperature there is a weakly first-order phase transition into a ferroelec- tric phase, as reported by Gesi (1990); this author has also pointed out the improper ferroelectric character of the phase transition.

In a preliminary X-ray diffraction study of TMCB (Aguirre-Zamalloa et al., 1990) the space groups of both room-temperature $[P6_3/m\ (Z = 2)]$ and low- temperature $[P6_1-P6_5\ (Z = 6)]$ phases have been established; in particular, the low-temperature ferro- electric phase is related to the room-temperature paraelectric phase by a tripling of the paraelectric lattice constant c (hexad direction), which replaces the point $\Delta(0,0,\frac{1}{3})$ situated inside the hexagonal $P6_3/m$ Brillouin zone (Bradley & Cracknell, 1972) at the zone centre in the ferroelectric phase. Further- more, a phenomenological approach based on Landau theory neatly fitted the static properties of this system across a first-order improper ferroelectric transition (Aguirre-Zamalloa et al., 1990). According to this description, the primary order parameter belongs to the $\Delta_2\Delta_3/E_1$ irreducible representation and is responsible for the tripling of the unit cell, while a secondary order parameter with Γ_1^-/A_u symmetry accounts for the spontaneous polarization observed along c (Gesi, 1990).

Recently, Krishnan et al. (1991) have determined the crystal structure of TMCB at room temperature. The space group $P6_3/m$ ($Z = 2$) has been confirmed, but, according to these authors, the R factor is not good enough because of the difficulties in *handling the dynamics of the TMA cation in the structure determination*. As a conclusion they argued that a disordered arrangement of the TMA cation must be assumed. Nevertheless, it should be noticed that the occupation probabilities for the disordered C atoms of the TMA group, such as assigned by Krishnan et al. (1991), merely comply with stoichiometry but do not allow any description of an orientationally dis- ordered tetrahedron.

In the present paper, we are concerned with the study and modelling of this disorder. We have repeated X-ray diffraction measurements at room temperature in order to confirm or restate the pre- vious results of Krishnan et al. (1991), and we have also determined the crystal structure of TMCB in the low-temperature ferroelectric phase with two main purposes:

(i) to clarify the ordering mechanism of the TMA groups and discuss it in terms of a suitable model;

(ii) to understand the physical origin of ferro- electricity.

2. Experimental

Colourless single crystals of TMCB were grown at room temperature by slow evaporation of a saturated aqueous solution containing $(CH_3)_4NBr$ and $CdBr_2$ in stoichiometric proportions. Small needles, elongated along the c direction, were selected for X-ray diffraction measurements.

Table 1. *Summary of crystal data and data-collection parameters*

Crystal form	Polyhedral	
Crystal size (mm)	0.48 × 0.43 × 0.55	
Temperature (K)	295	85.0 (2)
Reflections for lattice-parameter refinement	25 ($5.8 < \theta < 21.5°$)	16 ($5.8 < \theta < 21°$)
a (Å)	9.388 (2)	9.219 (4)
c (Å)	6.991 (5)	20.86 (1)
$(\sin\theta/\lambda)_{max}$ (Å^{-1})	0.703	0.703
h,k,l limits	0/13, −13/13, −9/9	−12/12, −12/12, −29/29
Scan type	θ–2θ	θ–2θ
Scan width (°)	0.70 + 0.35tanθ	
Scan speed range (" min^{-1})	0.72/4.12	
Measured reflections	3383	9916
Independent reflections	564	2961
R_{int}	0.118	0.082
Observed reflections [$I > 3\sigma(I)$]	435	2741
Transmission (min./max.)	0.024/0.065	0.034/0.065
Weighting scheme	$1/\sigma^2(F)$	$1/\sigma^2(F)$
No. of variables	26	119
No. of contributing reflections	518	2880
Max. shift/e.s.d.	0.18	0.04

The paraelectric phase has been studied at 295 K and the ferroelectric phase at 85 K. In both cases the intensities were collected from the same crystal. Data collection was performed using a CAD-4 diffractometer equipped with a nitrogen-gas-flow cooling system (Cosier & Glazer, 1986). Temperature stability was ±0.2 K during the measurement at 85 K. Monochromated Mo $K\alpha$ radiation was used in all experiments.

The observed systematic absences of reflections in both phases were compatible with the space groups previously determined ($P6_3/m$ and $P6_1$–$P6_5$, respectively). At 85 K Friedel pairs were measured to cope with the theoretically possible presence of enantiomorphic ($P6_1$–$P6_5$) twin domains or, if possible, to establish the absolute configuration of the low-temperature structure. During both measurements three check reflections were measured every 2 h without significant variation. Crystal data and data-collection parameters are summarized in Table 1.

3. Structure refinement

Data reduction and refinement were carried out with the *XRAY*72 system (Stewart, Kruger, Ammon, Dickinson & Hall, 1972). The intensities were corrected for Lorentz and polarization factors. An absorption correction was performed by the Gaussian-integration method. Atomic scattering factors of neutral Br, Cd, N, C and H atoms and anomalous-dispersion terms for Br and Cd were taken from *International Tables for X-ray Crystallography* (1974, Vol. IV, pp. 55, 99, 149). All the refinements were based on $|F|$, in full-matrix mode. Plots of the structures were prepared using the programs *SCHAKAL*88 (Keller, 1989) and *ORTEP* (Johnson, 1971).

3.1. *The paraelectric phase*

Cd, N and Br atoms were placed at the sites 2(b) (0,0,0), 2(c) ($\frac{1}{3},\frac{2}{3},\frac{1}{4}$) and 6($h$) ($x,y,\frac{1}{4}$) respectively; the starting coordinates x and y of Br atoms were those determined previously by Krishnan *et al.* (1991). Successive difference Fourier syntheses revealed the C atoms. After several anisotropic cycles, the refinement converged to an R (wR) value of 0.062 (0.075) for 435 observed reflections. The goodness of fit was 9.96. No attempt was made to locate the H atoms. A final difference synthesis showed peaks below 1.2 e Å^{-3}. Final positional coordinates and anisotropic thermal parameters of the paraelectric phase are reported in Table 2.* Fig. 1 represents a projection of the structure along c. Fig. 2 shows the configuration of the TMA groups, with disordered C atoms exhibiting very large thermal ellipsoids which will be discussed later.

The atomic coordinates obtained (see Table 2) compare well with those previously reported by Krishnan *et al.* (1991). Nevertheless, our results are better suited to the discussion of the orientational disorder of the TMA groups. On the one hand, knowledge of the anisotropic thermal parameters permits a better analysis of the TMA group's motion and, therefore, the modelling of the observed disorder. On the other hand, the occupation probabilities assigned to the C atoms (Table 2) suggest a model in which the tetrahedra are reoriented.

3.2. *The ferroelectric phase*

Starting coordinates for the Cd and Br atoms were extrapolated from those found in the paraelectric phase. $P6_5$ was the space group chosen for the refinement. The origin was fixed with an additional least-squares restraint according to Flack & Schwarzenbach (1988). Successive Fourier difference maps revealed that the N atoms and the surrounding C atoms were in a nearly perfect tetrahedral environment. In addition an enantiomorph-polarity parameter (Flack, 1983) was refined.

Final Fourier difference maps showed several maxima of about 1 e Å^{-3} in the neighbourhood of the C atoms. These residual peaks were assigned to H atoms and their positions refined using, as additional observations, soft restrictions for the C—H bond lengths. The temperature factors of all H atoms were considered isotropic and fixed at a reasonable value of 0.04 Å^2. Final R and wR values were 0.029 and 0.038, respectively. The goodness of fit was 2.2.

Table 2. *Atomic parameters of the paraelectric phase at* 295 K

PP is the population parameter. The temperature factor has the form of $\exp(-T)$, where $T = 2\pi^2\Sigma_{i,j}h_ih_jU_{ij}a_i{}^*a_j{}^*$ for anisotropic atoms. $a_i{}^*$ (i = 1, 2, 3) are the reciprocal axial lengths and h_i Miller indices. The e.s.d. of the last significant digit is given in parentheses.

	x	y	z	PP	U_{11}	U_{22}	U_{33}	U_{12}	U_{13}	U_{23}
Cd	0	0	0	1	0.0437	0.0437	0.0165 (7)	0.0219 (3)	0	0
Br	0.2651 (2)	0.1581 (2)	0.25	1	0.0351 (6)	0.0472 (7)	0.0298 (6)	0.0150 (5)	0	0
N	0.3333	0.6666	0.25	1	0.0308	0.0308	0.033 (9)	0.015 (2)	0	0
C(1)	0.150 (4)	0.522 (5)	0.25	½	0.04 (2)	0.10 (3)	0.22 (5)	-0.01 (2)	0	0
C(2)	0.223 (7)	0.580 (8)	0.094 (5)	½	0.17 (6)	0.17 (7)	0.03 (2)	0.06 (4)	-0.06 (3)	-0.04 (3)

Flack's parameter reached a final value of 0.50 (1) which indicates an equal proportion of the two, $P6_1$ or $P6_5$, configurations, in complete agreement with the practically equal intensity showed by the collected Friedel pairs.

Final atomic parameters of the ferroelectric phase are reported in Table 3.* Relevant interatomic distances and angles are listed in Table 4. Figs. 3(*a*) and 3(*b*) show the structure of the octahedra chains projected along **c** and **a** respectively. The arrangement of the TMA tetrahedra is represented in Fig. 4. The major characteristics of the ferroelectric phase concern the orientational ordering of the TMA cations (see Fig. 4), and the helical shape of the octahedra chains (Fig. 3*a*).

4. Discussion

As mentioned already, the phase transition observed in TMCB implies an ordering process of the TMA groups as well as small atomic displacements leading, in particular, to the helical shape of the octahedra chains. In fact, Raman-scattering experiments performed with TMCB through this phase transition (Aguirre-Zamalloa & Couzi, 1993) do not reveal any soft-mode behaviour, but show drastic changes in the linewidth of the Raman-active phonon modes. As a matter of fact, this type of behaviour is quite similar to that observed in other compounds of this family, such as TMMC and TMCC (see, *e.g.*, Peercy *et al.*,

* See deposition footnote.

Fig. 1. Projection along **c** of the structure at 295 K, showing the octahedral coordination of Cd atoms.

1973; Braud, Couzi, Chanh & Gómez-Cuevas, 1990). Thus, it can be safely stated that the driving force for the phase transitions occurring in all these compounds, including TMCB, is a result of order–disorder phenomena connected to the reorientational dynamics of the TMA groups, and that the small displacive contributions are 'secondary' effects as a result of couplings (linear or non-linear) of order–disorder processes with phonons. In this section, we shall first discuss the ordering process of the TMA groups in TMCB, then we shall consider the coupling with phonons responsible for the existence of helical octahedra chains, and finally, on the basis of the present structural study, we shall determine the physical origin of the ferroelectricity. To do this, we shall refer to a study of the symmetry properties of all phonon modes and pseudo-spin coordinates together with their compatibility relations in the two phases of TMCB, which will be published elsewhere (Aguirre-Zamalloa & Couzi, 1993). Thus, we do not intend to enter into the details of this group theoretical treatment, we shall just stress important points directly related to the transition mechanism.

4.1. *Order–disorder processes of the TMA groups*

The orientational disorder of the TMA groups in the paraelectric phase merely derives from the fact that the site point-group symmetry ($\bar{6}$) is not a subgroup of the molecular point group ($\bar{4}3m$) of the free TMA group. It follows that the symmetry elements of $\bar{6}$ (3, m_z or both) must be achieved statistically in space and time by superimposition of different orientations of the TMA groups. A convenient way to describe orientational disorder in
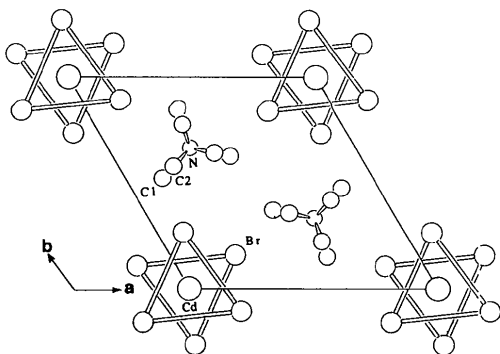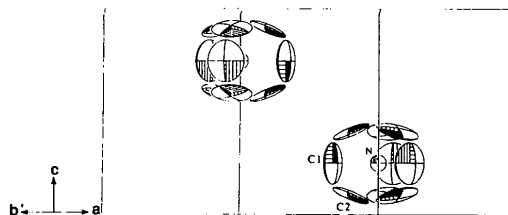

Fig. 2. Projection along [120] of the disordered $(CH_3)_4N$ groups in the paraelectric phase, showing the large thermal ellipsoids of C atoms. The axis labelled as b' is actually the projection of the b axis onto the projection plane.

Table 3. *Atomic parameters of the ferroelectric phase at* 85 K

The temperature factor has the form of $\exp(-T)$, where $T = 8\pi^2 U[(\sin\theta)/\lambda]^2$ for isotropic atoms, and $T = 2\pi^2\Sigma_{i,j}h_ih_jU_{ij}a_i{}^*a_j{}^*$ for anisotropic atoms. $a_i{}^*$ are the reciprocal axial lengths and h_i are Miller indices. The e.s.d. of the last significant digit is given in parentheses.

	x	y	z	U_{11} (or U)	U_{22}	U_{33}	U_{12}	U_{13}	U_{23}
Cd	0.00211 (6)	0.02445 (5)	-0.0009 (1)	0.0112 (2)	0.0122 (2)	0.0036 (2)	0.0056 (2)	-0.0008 (1)	-0.0004 (2)
Br(1)	0.28003 (7)	0.19652 (7)	0.0759 (1)	0.0099 (2)	0.0114 (2)	0.0057 (3)	0.0045 (2)	-0.0002 (2)	0.0002 (2)
Br(2)	-0.13849 (7)	0.14069 (7)	0.0900 (1)	0.0130 (3)	0.0145 (2)	0.0063 (3)	0.0086 (2)	-0.0006 (2)	0.0000 (2)
Br(3)	-0.08507 (7)	-0.24476 (6)	0.0815 (1)	0.0124 (3)	0.0111 (2)	0.0067 (2)	0.0062 (2)	-0.0001 (2)	0.0000 (2)
N	0.3483 (6)	0.6903 (5)	0.0814 (3)	0.010 (2)	0.010 (2)	0.011 (2)	0.005 (2)	0.001 (2)	0.004 (2)
C(1)	0.5066 (7)	0.6807 (7)	0.0878 (3)	0.013 (3)	0.016 (2)	0.029 (4)	0.009 (2)	-0.001 (3)	0.002 (3)
C(2)	0.3927 (8)	0.8726 (7)	0.0822 (4)	0.024 (3)	0.009 (2)	0.035 (4)	0.011 (2)	0.006 (3)	0.005 (3)
C(3)	0.2630 (9)	0.610 (1)	0.0196 (3)	0.025 (3)	0.034 (4)	0.016 (4)	0.015 (3)	-0.014 (3)	-0.013 (3)
C(4)	0.2319 (9)	0.6012 (9)	0.1360 (3)	0.028 (3)	0.023 (3)	0.017 (3)	0.012 (3)	0.011 (3)	0.008 (3)
H(11)	0.55 (1)	0.71 (1)	0.048 (2)	0.04					
H(12)	0.56 (1)	0.73 (1)	0.124 (3)	0.04					
H(13)	0.47 (1)	0.566 (3)	0.087 (5)	0.04					
H(21)	0.44 (1)	0.91 (1)	0.044 (3)	0.04					
H(22)	0.45 (1)	0.92 (1)	0.118 (3)	0.04					
H(23)	0.32 (1)	0.87 (1)	0.109 (4)	0.04					
H(31)	0.327 (9)	0.68 (1)	-0.014 (4)	0.04					
H(32)	0.24 (1)	0.509 (5)	0.038 (5)	0.04					
H(33)	0.173 (9)	0.62 (1)	0.026 (5)	0.04					
H(41)	0.20 (1)	0.492 (4)	0.136 (5)	0.04					
H(42)	0.29 (1)	0.68 (1)	0.168 (3)	0.04					
H(43)	0.140 (8)	0.61 (1)	0.127 (5)	0.04					

Table 4. *Selected interatomic distances* (Å) *and angles* (°) *of the ferroelectric phase at* 85 K

The e.s.d. of the last significant digit is given in parentheses.

Cd—Br(1)	2.754 (2)	Br(1)—Cd—Br(2)	81.99 (7)
Cd—Br(2)	2.795 (2)	Br(1)—Cd—Br(3)	85.69 (8)
Cd—Br(3)	2.787 (2)	Br(2)—Cd—Br(3)	86.58 (8)
N—C(1)	1.51 (1)	C(1)—N—C(2)	109.3 (4)
N—C(2)	1.518 (8)	C(1)—N—C(3)	109.2 (6)
N—C(3)	1.50 (1)	C(1)—N—C(4)	110.4 (6)
N—C(4)	1.498 (9)	C(2)—N—C(3)	110.1 (6)
C(1)—H(11)	0.91 (6)	C(2)—N—C(4)	108.7 (6)
C(1)—H(12)	0.91 (6)	C(3)—N—C(4)	109.2 (4)
C(1)—H(13)	0.93 (3)		
C(2)—H(21)	0.90 (6)		
C(2)—H(22)	0.90 (7)		
C(2)—H(23)	0.9 (1)		
C(3)—H(31)	0.92 (8)		
C(3)—H(32)	0.91 (7)		
C(3)—H(33)	0.9 (1)		
C(4)—H(41)	0.90 (5)		
C(4)—H(42)	0.91 (7)		
C(4)—H(43)	0.9 (1)		

molecular crystals is the Frenkel model, in which the molecules (TMA groups in our case) execute jumps between a finite number of equiprobable orientations. Such a description permits the introduction of pseudo-spin variables that can be easily handled with the help of classical group-theoretical techniques in the frame of the Landau theory (see, *e.g.*, Couzi, Negrier, Poulet & Pick, 1988). The freezing of such pseudo-spin coordinates is related with the ordered states that can be obtained in low-temperature phases. Of course, such a description is an oversimplification in those cases where the experimental results rather suggest the existence of continuous distributions of orientations (Pauling model).

In the case of TMCB and related compounds, different models of the Frenkel type can be considered.

(i) A two-well model (2W) in which one threefold axis of the TMA tetrahedron coincides with the threefold axis in the site, so that the m_z mirror plane

is achieved statistically by superimposition of two equiprobable orientations related to each other by the m_z symmetry operation (Morosin & Graeber, 1967; Morosin, 1972; Peercy *et al.*, 1973).

(ii) A three-well model (3W) in which one mirror plane of the TMA tetrahedron coincides with the m_z mirror plane, so that the threefold axis of the site is statistically achieved by superimposition of three equiprobable orientations (Jewess, 1982).
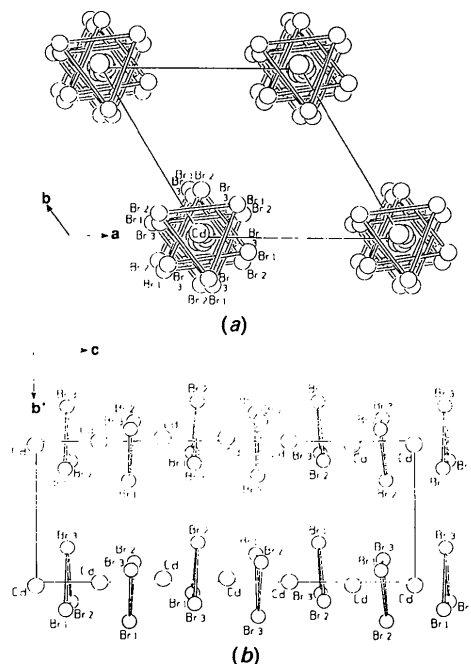

Fig. 3. (*a*) Projection of the octahedra chains along c in the ferroelectric phase. (*b*) Projection of the octahedra chains along a. The axis labelled as *b'* is actually the projection of the *b* axis onto the projection plane.

(iii) A six-well model $(6W)$ in which the TMA groups are in instantaneous general positions, so that both the 3 and m_z of the site are statistical elements of symmetry generated by superimposition of six equiprobable orientations (Couzi & Mlik, 1986).

The $2W$ model cannot be applied in the case of TMCB, since no electronic density has been detected along the threefold axis (Fig. 2).

From the point of view of symmetry, the $3W$ model plays a prominent role in the explanation of all phase sequences observed in the related compounds TMMC and TMCC (Braud, Couzi & Chanh, 1990); in particular, the existence of a monoclinic phase in these crystals with $P2_1/m$ $(Z = 2)$ space group, where the TMA groups are ordered in m_z sites, is at variance with both the $2W$ and $6W$ models, but fits exactly the $3W$ model. Hence, this latter seems to present some kind of 'universality' in this family of compounds.

In this context, let us examine to what extent the $3W$ model is or is not suitable in the case of TMCB. First of all, it should be noted that the orientationally ordered state of TMA groups observed in the ferroelectric phase (Fig. 4) is that expected for the $3W$ model, although there is a small misorientation ($\sim 5.6°$) between the ab plane and the plane defined by the N atom and the two equatorial C atoms [C(1) and C(2) in Table 3]. Indeed, the $3W$ model has a pseudo-spin coordinate with $\Delta_2\Delta_3/E_1$ symmetry (primary order parameter); this four-dimensional representation in $P6_3/m$ (Bradley & Cracknell, 1972) can induce at point $\Delta(0,0,\frac{1}{3})$ different space groups for the low-temperature phase, namely $P6_1–P6_5$, $P2_1/m$ or $P2_1$ with $Z = 6$ (Aguirre-
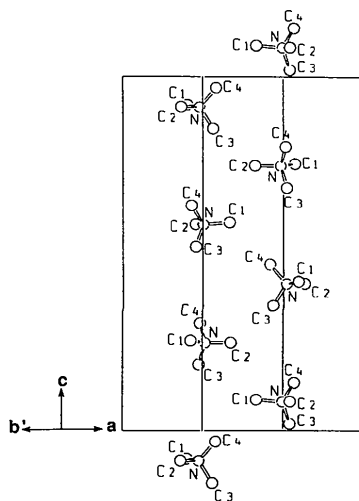
Zamalloa & Couzi, 1993). In the case of the observed $P6_1–P6_5$ space group, the freezing of this pseudo-spin coordinate corresponds to an *ordered* state where the TMA groups are oriented alternately along the **c** direction according to one of the three equivalent orientations in the $P6_3/m$ space group. This fits nicely the experimental results (see Fig. 4) in the ferroelectric phase and is related with the tripling of the paraelectric lattice parameter c. In this phase, the TMA tetrahedra are nearly regular (see Table 4). Their small tilt (about 5.6°) can easily be explained by the freezing of a rotatory mode of the TMA groups (around axes which are perpendicular to c) which also belongs to the $\Delta_2\Delta_3/E_1$ representation and, therefore, can be linearly coupled with the pseudo-spin variable.

The situation in the paraelectric phase is much less clear as we have to extract several discrete C-atom positions from their large thermal ellipsoids (Fig. 2). As is shown in Fig. 5, this can easily be performed on the m_z mirror plane, since in the $3W$ model the angle made by the nearest equatorial atoms [C(1) with occupation probabilities of $\frac{1}{3}$ in Fig. 5a] is $\sim 10.5°$. We can reasonably expect that, when thermally agitated, these atoms merge into an average atomic 'cloud' with a occupancy of $\frac{2}{3}$ (Fig. 5b). Actually, this is the way in which the structure at 295 K has been refined. However, the refined model has several drawbacks. On the one hand, the TMA
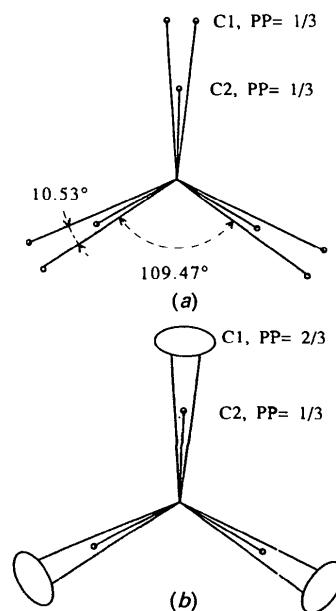

Fig. 4. Projection along [120] of the ordered $(CH_3)_4N$ groups in the ferroelectric phase. The H atoms have been omitted for clarity. The axis labelled as b' is actually the projection of the b axis onto the projection plane.

Fig. 5. (a) Scheme of the atomic positions issued from the $3W$ model with the statistical threefold axis perpendicular to the plane of the figure. Note the splitting of the C(1)-atom positions with occupancy of $\frac{1}{3}$. (b) Same as (a), but with non-split C(1) positions and an occupancy of $\frac{2}{3}$.

Table 5. *Symmetry-independent interatomic distances (Å) and angles (°) of one disordered TMA unit in the paraelectric phase at 295 K*

The e.s.d. of the last significant digit is given in parentheses.

N—C(1)	1.56 (9)	N—C(2)	1.44 (4)
C(2)—C(1')	2.45 (6)	C(2)—N—C(1')	109 (3)
C(2)—C(2")	2.18 (5)	C(2)—N—C(2")	98 (3)
C(2)—C(1''')	2.46 (8)	C(2)—N—C(1''')	109 (3)
C(1')—C(1''')	2.72 (6)	C(1')—N—C(1''')	120 (2)

Symmetry operations: (i) $y - x$, $1 - x$, z; (ii) x, y, $\frac{1}{2} - z$; (iii) $1 - y$, $1 - y + x$, z.

tetrahedron is much more distorted than that found in the ferroelectric phase (see Table 5). Strictly speaking it exhibits distances which are too long [N—C(1)] and too short [N—C(2)]. On the other hand, the very large thermal component U_{33} (out of the mirror plane) of the C(1) atoms [which are strongly correlated with the thermal motion of the C(2) atoms as can be deduced from Fig. 2] should be carefully analysed. Hence the $3W$ model appears to be highly 'perturbed' by these large-amplitude librations out of the plane which are present in the paraelectric phase of TMCB.

At this stage, another (more complex) structural model was tried. One of the low-temperature ordered tetrahedra was placed in the paraelectric structure; its centre (the N atom) was located at a $\bar{6}$ site whereas the C atoms occupied general positions. In addition the tetrahedron was forced, by very strong soft restrictions, to be perfectly rigid. C atoms were refined isotropically and their temperature factors were restricted (see Table 6 and Figs. 2 and 4) in such a way that the large thermal ellipsoid of each C atom in the paraelectric phase was decomposed into four identical parts. The refinement process converged quickly into a $6W$ model. The final R (wR) factor was 0.064 (0.079). The atomic parameter list is given in Table 6.* Nevertheless in the refined tetrahedron, the plane defined by the N, C(1) and C(2) atoms makes an angle of $\sim 16.4°$ with respect to the ab plane. This rather large tilt angle evidently means that the low-temperature positions are far from any of these frozen orientations. Furthermore, it should be noted that a freezing of the $6W$ model into the ordered state involves simultaneously at least two pseudo-spin coordinates with $\Delta_2\Delta_3/E_1$ and Γ_1^-/A_u symmetry, respectively. This non-linear coupling obviously leads to a much more complex ordering mechanism than that inferred from the $3W$ model. On the other hand, the overall agreement (measured by the R factor) for the paraelectric phase is rather insensitive to the details of the different models proposed as can be concluded from the almost spherical distribution of TMA groups shown in Fig. 2.

---

* See deposition footnote.

Summarizing, the 'perturbed' $3W$ model seems to provide the best description (or at least the simplest one) for the ordering processes of the TMA tetrahedra in TMCB, though the $6W$ model cannot be completely ruled out. Indeed, we are reaching the limits of a Frenkel-type description and we cannot, in the present case, choose between the two models in the absence of additional information.

4.2. *Helical structure of the octahedra chains*

The octahedra chains exhibit a helical shape in the ferroelectric phase (see Fig. 3a), since both Cd and Br atoms have been slightly moved, perpendicularly to c, from the positions occupied in the paraelectric phase; the same is true for the N atoms, i.e. the approximate centres of mass of the TMA groups (see Tables 2 and 3).

This configuration can be easily understood by the freezing of the transverse acoustic mode [TA(Δ)] at point $\Delta(0,0,\frac{1}{3})$, together with the pseudo-spin coordinates described in §4.1. Indeed, the frozen-in atomic displacements of TA(Δ) leading to $P6_1-P6_5$, result in a helically distorted structure with a pitch of three times the paraelectric axial length c.

Moreover, note that the normals to the planes defined by the three nearest Br atoms are tilted ($\sim 4.7°$) with respect to the c axis (Fig. 3b). Again, this can be explained by assuming the freezing of an optical mode at point $\Delta(0,0,\frac{1}{3})$ (with Δ_2, Δ_3/E_1 symmetry). This mode does not change the z coordinates of the 'mean' Br planes defined by the averaged individual z coordinates of these Br atoms.

Therefore, the distorted structure can be thoroughly described by the pseudo-spin coordinates (the primary-order parameter of the transition with $\Delta_2,\Delta_3/E_1$ symmetry) and small additional contributions (bi-linear couplings) coming from both the transverse acoustic mode and an optical mode; probably, these particular phonons will 'assist' the ordering processes of the TMA groups so that a pseudo-spin phonon-coupled mechanism can be inferred.

4.3. *Spontaneous polarization*

The spontaneous polarization along the c axis (P_z) allowed by the symmetry in the low-temperature phase of TMCB has been measured by Gesi (1990). Its value at 125 K ($P_z \simeq 1.2 \times 10^{-3}$ C m^{-2}), indicates that TMCB is a rather weak ferroelectric compound corresponding to an improper ferroelectric compound in which P_z is a secondary order parameter (Aguirre-Zamalloa *et al.*, 1990).

In the ferroelectric phase the ordered TMA groups are slightly distorted from a perfect tetrahedral symmetry and, therefore, may carry a permanent dipole moment. Using the atomic coordinates for N, C and

Table 6. *Atomic parameters of the paraelectric phase at* 295 K *obtained with the* 6W *model* (*see text*) *for rigid* $(CH_3)_4N$ *entities*

PP is the population parameter. The temperature factor has the form of $\exp(-T)$, where $T = 8\pi^2 U[(\sin\theta)/\lambda]^2$ for isotropic atoms, and $T = 2\pi^2 \Sigma_{i,j} h_i h_j U_{ij} a_i^* a_j^*$ for anisotropic atoms. a_i^* are reciprocal axial lengths and h_i are Miller indices. The e.s.d. of the last significant digit is given in parentheses.

	x	y	z	PP	U_{11} (or U)	U_{22}	U_{33}	U_{12}	U_{13}	U_{23}
Cd	0	0	0	1	0.0437	0.0437	0.016 (4)	0.022 (2)	0	0
Br	0.2653 (9)	0.1582 (9)	0.25	1	0.035 (4)	0.047 (4)	0.030 (4)	0.015 (3)	0	0
N	0.3333	0.6666	0.25	1	0.0288	0.0288	0.03 (2)	0.014 (4)	0	0
C(1)	0.479 (5)	0.648 (8)	0.30 (6)	$\frac{1}{6}$	0.07 (2)					
C(2)	0.392 (8)	0.844 (3)	0.201 (8)	$\frac{1}{6}$	0.07 (2)					
C(3)	0.244 (4)	0.558 (5)	0.083 (3)	$\frac{1}{6}$	0.08 (3)					
C(4)	0.218 (3)	0.617 (7)	0.417 (3)	$\frac{1}{6}$	0.08 (3)					

H given in Table 3, a semi-empirical calculation based on the $AM1$ Hamiltonian method leads to a permanent dipole moment, for the distorted TMA groups, of ~ 0.29 D (9.6734×10^{-31} C m), the z component of which is $m_z \simeq 0.27$ D (9.0062×10^{-31} C m) (Gorse, Liotard & Pesquer, 1992). Although this value represents a (positive) contribution to P_z of the correct order of magnitude (*i.e.* between 10^{-2} and 10^{-3} C m^{-2}), it has to be considered with caution, given the large uncertainties affecting the H-atom positions (Table 3).

On the other hand, taking in both phases the position of one Cd atom as the origin along the c direction, it can be easily established from Tables 2 and 3 that, within the limits of the experimental accuracy, the z coordinate of the 'mean' Br planes is the same in both (high- and low-temperature) phases whereas the TMA groups as a whole have moved by ~ 0.022 Å in the negative sense. Clearly, these shifts in atomic positions along c describe a displacement of the inorganic chains (negatively charged) with respect to the TMA groups (positively charged), and create another contribution to P_z. A crude estimate of this contribution by means of a point-charge model with fully ionized particles, namely Cd^{2+}, Br^- and TMA^+, again lies within the range of 10^{-3} C m^{-2}, but with a negative sign according to the adopted convention.

Therefore, the spontaneous polarization P_z can be described as the result of two competing contributions with opposite signs. The first comes from the internal distortion of the ordered TMA groups, whereas the second is as a result of relative translations, along the c axis, between the inorganic chains and the TMA groups as a whole.

References

Aguirre-Zamalloa, G. & Couzi, M. (1993). In preparation.
Aguirre-Zamalloa, G., Couzi, M., Chanh, N. B. & Gallois, B. (1990). *J. Phys.* **51**, 2135–2141.
Alcock, N. W. & Holt, S. L. (1978). *Acta Cryst.* B**34**, 1970–1972.
Bradley, C. J. & Cracknell, A. P. (1972). *The Mathematical Theory of Symmetry in Solids.* Oxford: Clarendon Press.
Braud, M. N., Couzi, M. & Chanh, N. B. (1990). *J. Phys. Condens. Matter*, **2**, 8243–8258.
Braud, M. N., Couzi, M., Chanh, N. B., Courseille, C., Gallois, B., Hauw, C. & Meresse, A. (1990). *J. Phys. Condens. Matter*, **2**, 8209–8228.
Braud, M. N., Couzi, M., Chanh, N. B. & Gómez-Cuevas, A. (1990). *J. Phys. Condens. Matter*, **2**, 8229–8242.
Cosier, J. & Glazer, A. M. (1986). *J. Appl. Cryst.* **19**, 105–107.
Couzi, M. & Mlik, Y. (1986). *J. Raman Spectrosc.* **17**, 117–124.
Couzi, M., Negrier, Ph., Poulet, H. & Pick, R. M. (1988). *Croat. Chem. Acta*, **61**, 649–670.
Flack, H. D. (1983). *Acta Cryst.* A**39**, 867–881.
Flack, H. D. & Schwarzenbach, D. (1988). *Acta Cryst.* A**44**, 499–506.
Gesi, K. (1990). *J. Phys. Soc. Jpn*, **59**, 432–434.
Gorse, D., Liotard, D. & Pesquer, M. (1992). Private communication.
Guillaume, F., Couzi, M. & Bée, M. (1992). *Physica*, B**180–181**, 714–716.
Jewess, M. (1982). *Acta Cryst.* B**38**, 1418–1422.
Johnson, C. K. (1971). *ORTEPII.* Report ORNL-3794, revised. Oak Ridge National Laboratory, Tennessee, USA.
Keller, E. (1989). *J. Appl. Cryst.* **18**, 258–262.
Krishnan, V. G., Dou, S. & Weiss, A. (1991). *Z. Naturforsch. Teil A*, **46**, 1063–1082.
Mangum, B. W. & Utton, D. B. (1972). *Phys. Rev. B*, **6**, 2790–2796.
Morosin, B. (1972). *Acta Cryst.* B**28**, 2303–2305.
Morosin, B. & Graeber, E. J. (1967). *Acta Cryst.* **23**, 766–770.
Peercy, P. S., Morosin, B. & Samara, G. A. (1973). *Phys. Rev. B*, **8**, 3378–3388.
Stewart, J. M., Kruger, G. J., Ammon, H. L., Dickinson, C. & Hall, S. R. (1972). The *XRAY* system – version of June 1972. Tech. Rep. TR-192. Computer Science Center, Univ. of Maryland, College Park, Maryland, USA.
Tsang, T. & Utton, D. B. (1976). *J. Chem. Phys.* **64**, 3780–3783.
Vanek, P., Havranova, M., Smutny, F. & Brezina, B. (1990). *Ferroelectrics*, **109**, 51–56.
Visser, D. & McIntyre, G. J. (1989). *Physica*, B**156–157**, 259–262.